Effects of magnetic field on photon-induced quantum transport in a single dot-cavity system

Nzar Rauf Abdullah[1,2,†], Aziz H Fatah[1], and Jabar M A Fatah[1]

[1] *Physics Department, College of Science, University of Sulaimani, Kurdistan Region, Iraq*
[2] *Science Institute, University of Iceland, Dunhaga* 3, *IS*-107 *Reykjavik, Iceland*

(Received 2 April 2016; revised manuscript received 25 June 2016; published online 30 September 2016)

In this study, we show how a static magnetic field can control photon-induced electron transport through a quantum dot system coupled to a photon cavity. The quantum dot system is connected to two electron reservoirs and exposed to an external perpendicular static magnetic field. The propagation of electrons through the system is thus influenced by the static magnetic and the dynamic photon fields. It is observed that the photon cavity forms photon replica states controlling electron transport in the system. If the photon field has more energy than the cyclotron energy, then the photon field is dominant in the electron transport. Consequently, the electron transport is enhanced due to activation of photon replica states. By contrast, the electron transport is suppressed in the system when the photon energy is smaller than the cyclotron energy.

Keywords: cavity quantum electrodynamics, electronic transport in mesoscopic systems, quantum interference devices, magnetotransport phenomena

PACS: 42.50.Pq, 73.23.–b, 78.20.Jq, 75.47.–m **DOI:** 10.1088/1674-1056/25/11/114206

1. Introduction

Quantum dots (QDs) are a crucial electronic structure in technological devices[1–3] because of their unique properties, such as zero-dimensional confinement effect[4] and single electron charge effect (Coulomb blockade).[5] Several methods have been used to control electron motion in a QD system, one of which is to control the energy levels and the electron concentration in the QD systems using a plunger gate voltage.[6] On the other hand, applying a photon radiation that interacts with the electrons in the QD induces a fascinating physical phenomena called photon-assisted tunneling (PAT).[6,7] The PAT occurs in quantum systems when a photon radiation is applied to an electronic island connected to electron reservoirs.[8] The photon radiation forms extra channels in the electronic island, leading to a modification in the electron transport.[9] Therefore, the photon radiation can play an essential role in the transport process generating a photocurrent that depends on the photon frequency.[10] Recently, the influences of photon field, in a vacuum state, on two-level electronic system,[11] and double quantum dots in the presence of a single mode micro-cavity system with both continuous wave and pulsed excitation are studied.[12] Based on the proposed schemes, a single photon generation can be obtained separately under both QD–cavity resonant and off-resonant conditions. The single photon source, in turn, becomes increasingly important in the very diverse range of technological applications.

In addition, external magnetic fields can be used to control the electron transport in nanodevices, which leads to several important effects including the change of the energy level spacing inside the QD[13] and hence the QD lowest energy state shrinks with increasing magnetic field. As a result, the Coulomb interaction between two spin degenerate electrons grows.[14] Furthermore, external magnetic field can form the edge state[15] and the localized state[16] in the electronic systems, and consequently the electron transport is reduced.

The combination of the aforementioned fields, namely the magnetic and photon fields, can result in a magneto-photon current in graphene[17] and superconductor.[18] In this work, we consider magneto-photo transport under the influence of a quantized single photon mode in a cavity and investigated its effect on electron transport through a QD system. In the presence of the photon cavity, extra channels are formed in the system, which open new windows for electron tunneling called photon-assisted tunneling process. In addition, we have also shown how an external static magnetic field can control photon-assisted tunneling in the QD system.

The rest of this paper is organized as follows. In Section 2, the description of the model and the theoretical formalism are shown. In Section 3, we demonstrate the results. In Section 4, conclusions will be presented.

2. Model and theory

The system under investigation is a two-dimensional (2D) electron gas exposed to an external static magnetic field and a quantized photon field at low temperature. We assume that the electronic system consists of a QD embedded in a quantum wire. The QD system is connected to two electron reservoirs

†Corresponding author. E-mail: nzar.r.abdullah@gmail.com

© 2016 Chinese Physical Society and IOP Publishing Ltd

with different chemical potentials. The electron–photon coupling system is described by the following Hamiltonian in the many-body (MB) basis:

$$\hat{H} = \hat{H}_{\rm e} + \hat{H}_{\gamma} + \hat{H}_{\text{e-}\gamma}, \tag{1}$$

where $H_{\rm e}$ is the Hamiltonian of the electronic system including electron–electron interaction

$$\hat{H}_{\rm e} = \int {\rm d}r \hat{\psi}^{\dagger}(\boldsymbol{r}) \left[\frac{\boldsymbol{\pi}^2}{2m^*} + \frac{1}{2} m^* \Omega_0^2 y^2 + U_{\rm Dot} + eU_{\rm pg} \right] \hat{\psi}(\boldsymbol{r}) + \int {\rm d}r \int {\rm d}r' \hat{\psi}^{\dagger}(\boldsymbol{r}) \hat{\psi}^{\dagger}(\boldsymbol{r}') U_{\rm C}(\boldsymbol{r}, \boldsymbol{r}') \hat{\psi}(\boldsymbol{r}') \hat{\psi}(\boldsymbol{r}). \tag{2}$$

Herein, $\boldsymbol{\pi} = \boldsymbol{p} + (e/c)\boldsymbol{A}$ with $\boldsymbol{p}$ and $\boldsymbol{A} = -By\hat{\boldsymbol{x}}$ being the canonical momentum and magnetic vector potential, respectively. The magnetic field is applied along the z axis, i.e., $\boldsymbol{B} = B\hat{\boldsymbol{z}}$, and $\hat{\psi}(\boldsymbol{r}) = \sum_i \psi_i(r) d_i$ and $\hat{\psi}^{\dagger}(\boldsymbol{r}) = \sum_i \psi_i^*(r) d_i^{\dagger}$ are the fermionic field operators with d_i ($d_i^{\dagger}$) being the annihilation (creation) operators for an electron in the single electron state $|i\rangle$ corresponding to ψ_i. The QD potential can be described by

$$U_{\rm Dot} = U {\rm e}^{(-\alpha_x^2 x^2 - \alpha_y^2 y^2)}, \tag{3}$$

where U is the strength of the potential, and α_x and α_y are constants that determine the diameter of the QD. The plunger-gate voltage is described by $U_{\rm pg}$ which is an electrostatic potential shifting the energy states of the QD system with respect to the chemical potential of the leads. The second term of Eq. (2) indicates the electron–electron interaction in the central system with $U_{\rm C}$ being the Coulomb interaction potential.[19]

The second part of Eq. (1) can be written as $H_{\gamma} = \hbar\omega_{\gamma} a^{\dagger} a$ introducing the Hamiltonian of the free photon field with $\hbar\omega_{\gamma}$ being the photon energy, and a ($a^{\dagger}$) the photon annihilation (creation) operators. The quantized vector potential of the cavity photon field, in the Coulomb gauge, is given by $\hat{\boldsymbol{A}}_{\gamma} = A(\hat{a} + \hat{a}^{\dagger})\boldsymbol{e}$, where A is the amplitude of the photon field, related to the electron–photon coupling constant via $g_{\gamma} = eAa_w\Omega_w/c$, and $\boldsymbol{e}$ determines the photon polarization with either parallel $\boldsymbol{e} = \boldsymbol{e}_x$ or perpendicular $\boldsymbol{e} = \boldsymbol{e}_y$ to the electron motion. Note that a_w is the effective magnetic length and Ω_w is the effective confinement frequency of electrons of the QD system.

The last term on the right side of Eq. (1)

$$\hat{H}_{e\text{-}\gamma} = -\frac{1}{c} \int {\rm d}\boldsymbol{r}\, \boldsymbol{j}(\boldsymbol{r}) \cdot \boldsymbol{A}_{\gamma} - \frac{e}{2m^* c^2} \int {\rm d}\boldsymbol{r} \rho(\boldsymbol{r}) A_{\gamma}^2, \tag{4}$$

represents the full electron–photon interaction including both para- and dia-magnetic electron–photon interactions, respectively. The charge is $\rho = -e\psi^{\dagger}\psi$ and the charge current density is governed by

$$\boldsymbol{j} = -\frac{e}{2m^*} \left\{ \psi^{\dagger} (\boldsymbol{\pi}\psi) + (\boldsymbol{\pi}^* \psi^{\dagger}) \psi \right\}. \tag{5}$$

The electron–electron and the electron–photon interactions are treated by exact diagonalization in appropriately truncated Fock spaces.

Figure 1 shows the schematic diagram of the QD system (brown color) connected to two leads (black color) under the combined effects of the magnetic field B (red arrows) and the photon radiation (blue zigzag arrows). The chemical potential of the left lead $\mu_{\rm L}$ is assumed to be higher than that of the right lead $\mu_{\rm R}$. Consequently, the transport is dominated by the left to right electron motions between the two leads through the central system as indicated by violet arrows.

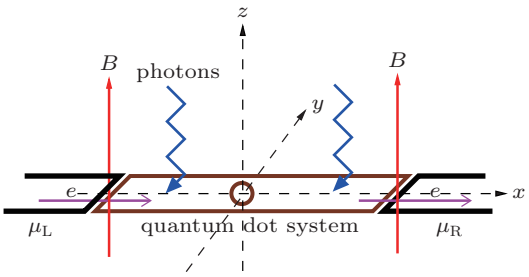


Fig. 1. (color online) Schematic diagram of a QD system (brown color) connected to the left lead (black color) with chemical potential $\mu_{\rm L}$ and and the right lead with chemical potential $\mu_{\rm R}$. The photon field is represented by the blue zigzag arrow. The external magnetic field B is labeled by the red arrow.

The Liouville–von Neumann equation is used to describe the time evolution of the many-body density operator of the closed system. However, in the case of open system when the central system is connected to the leads, we use a projection operator technique to derive a generalized master equation for the reduced density operator.[20,21] Since we are interested in the transient behavior of the system, we assume a non-Markovian approach valid to a weak coupling of the leads to the central system.[16]

Once we have the reduced density operator, one can calculate charge current and charge density in the system. The charge current is $I^{\rm c}(t) = I^{\rm L}(t) - I^{\rm R}(t)$, where $I^{\rm L}(t)$ indicates the partial current from the left lead into the QD system, and $-I^{\rm R}(t)$ refers to the partial current into the right lead from the QD system. The partial current can be introduced as $I^{\rm L,R} = {\rm Tr}[\dot{\hat{\rho}}_{\rm S}^{\rm L,R}(t)\hat{Q}]$, where $\dot{\hat{\rho}}_{\rm S}^{\rm L}$ and $\dot{\hat{\rho}}_{\rm S}^{\rm R}$ are the time derivatives of the system's reduced density matrix due to its coupling to the left and right leads, respectively,[19,22] and $\hat{Q} = e\hat{N}$ is the charge operator with the number operator $\hat{N}$.

3. Results and discussions

We assume the QD system and the leads are made of GaAs semiconductor with effective electron mass $m^* = 0.067m_{\rm e}$ and relative dielectric constant $\kappa = 12.4$. The parameters of the QD potential are $U = -3.3$ meV, and $\alpha_x = \alpha_y = 0.03$ nm^{-1}. The cavity consists of a single photon mode with energy $\hbar\omega_{\gamma} = 0.3$ meV, and the electron–photon coupling strength $g_{\gamma} = 0.1$ meV. The chemical potential of the left and the right leads are $\mu_{\rm L} = 1.2$ meV and $\mu_{\rm R} = 1.1$ meV, respectively, implying the bias voltage $\Delta\mu = \mu_{\rm L} - \mu_{\rm R} = 0.1$ meV. The

temperature of the leads before coupling to the QD system is $T = 0.001$ K. The confinement energy of electrons in the QD system is equal to that of the leads $\hbar\Omega_0 = \hbar\Omega_l = 2.0$ meV. Finally, the photon field is linearly polarized and aligned with the x axis parallel to the direction of electron motion in the QD system.

In what follows, we explain the influences of the magnetic field on photon-induced electron transport through the QD system. Figure 2 shows the energy spectrum of the QD system versus the plunger-gate voltage including zero-electron states (0ES, golden diamonds), one-electron states (1ES, blue rectangles), and two-electron states (2ES, red circles). The chemical potential of the leads are indicated by two horizontal lines (black lines).

In Fig. 2(a) the many-electron (ME) energy of the QD system, excluding the photon cavity, is demonstrated. For the selected range of the plunger-gate voltage, the first excited state lies between the two chemical potentials, inside the bias window, which in turn gets into resonance with the first sub-band energy of the leads located in the bias window. Therefore, an electron in the first sub-band of the left lead may perform electron tunneling into the first-excited state of the QD system. As a result, a peak in the charge current is formed at $U_{\rm pg}^0 = 0.4$ mV, as shown in Fig. 3. In addition, it should be known that the ground state energy of the QD system is found below 0.8 meV (not shown).

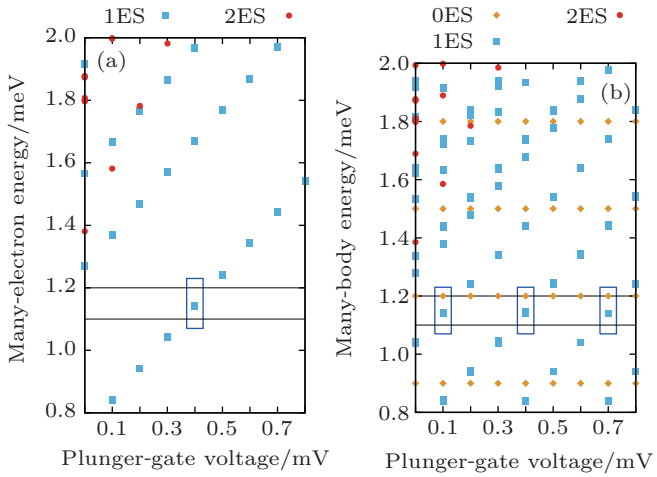


Fig. 2. (color online) The energy spectrum of the QD system without (a) and with (b) photon cavity versus the plunger-gate voltage $U_{\rm pg}$ including zero-electron states (0ES, golden diamonds), one-electron states (1ES, blue rectangles), and two-electron states (2ES, red dots). The chemical potentials are $\mu_{\rm L} = 1.2$ meV and $\mu_{\rm R} = 1.1$ meV (black). The SE state in the bias window is almost doubly degenerate due to the small Zeeman energy.

In Fig. 3(a) the charge current versus the plunger-gate voltage $U_{\rm pg}$ is plotted for three different values of the cyclotron energy $\hbar\omega_{\rm c} \simeq 10^{-4}$ meV (blue solid), 0.34 meV (green dashed), and 0.86 meV (red dotted), corresponding to the magnetic field $B = 0.0001$ T, 0.2 T, and 0.5 T, respectively. We can clearly see that the peak current increases with the cyclotron energy. At $\hbar\omega_{\rm c} \simeq 10^{-4}$ meV, the charge current is very weak. This can be attributed to the localization of charge density in the QD (see Fig. 4(a)). In contrast, for higher value of cyclotron energy (such as $\hbar\omega_{\rm c} \simeq 0.86$ meV) corresponding to the higher magnetic field, the charge is delocalized and slightly extended to the outside of the QD which can be understood as follows. The high magnetic field induces stronger Lorentz force that forms a circular motion of the electron charge density outside the dot (not shown), and consequently the charge current is enhanced (see the red dotted line in Fig. 3(a)).

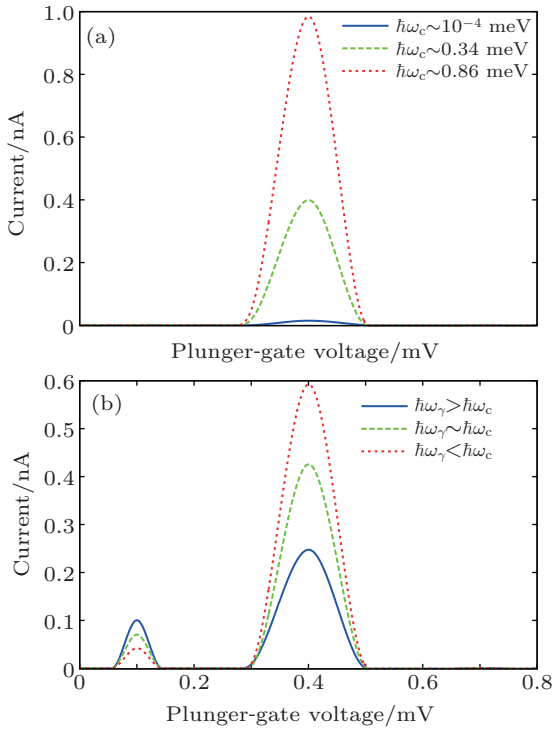


Fig. 3. (color online) The charge current $I_{\rm Q}$ is plotted as a function of plunger gate voltage $U_{\rm pg}$ at time $t = 220$ ps for (a) the QD system without photon cavity for cyclotron energy $\hbar\omega_{\rm c} \simeq 10^{-4}$ meV (blue solid), 0.34 meV (green dashed), and 0.86 meV (red dotted), and (b) the QD system with photon cavity for $\hbar\omega_\gamma > \hbar\omega_{\rm c}$ (blue solid), $\hbar\omega_\gamma \simeq \hbar\omega_{\rm c}$ (green dashed), and $\hbar\omega_\gamma < \hbar\omega_{\rm c}$ (red dotted), where the photon energy is $\hbar\omega_\gamma = 0.3$ meV. The bias window is $\Delta\mu = 0.1$ meV, $g_\gamma = 0.1$ meV, and $N_\gamma = 2$.

Now assuming the QD system is coupled to the cavity photon, the electron transport can be affected by both the static magnetic and the dynamic photon fields. For a photon energy $\hbar\omega_\gamma = 0.3$ meV and the electron–photon coupling strength $g_\gamma = 0.1$ meV, figure 2(b) demonstrates how the many-body (MB) energy varies as a function of the plunger-gate voltage. In the presence of the cavity, photon replica states are formed with different photon contents. The energy spacing between the photon replica states is appropriately equal to the photon energy at low electron–photon coupling strength. Therefore, the first excited state in the bias window is no longer active in the electron transport but instead the electrons from the left leads transfer to the photon replica of the first excited state in

the QD system. Comparing to the energy spectrum of the QD system in Fig. 2(a) for which the photon field is neglected, in Fig. 2(b) two photon replica states at $U_{pg} = 0.1$ and 0.7 mV (blue rectangles) are found in the bias window corresponding to $U_{pg} = U^0_{pg} - \hbar\omega_\gamma$ and $U_{pg} = U^0_{pg} + \hbar\omega_\gamma$, respectively.

Figure 3(b) shows the charge current as a function of the plunger-gate voltage in the presence of the photon cavity for three cases $\hbar\omega_\gamma > \hbar\omega_c$ (blue solid), $\hbar\omega_\gamma \simeq \hbar\omega_c$ (green dashed), and $\hbar\omega_\gamma < \hbar\omega_c$ (red dotted), where the photon energy is $\hbar\omega_\gamma = 0.3$ meV. The peak current (main peak) at $U^0_{pg} = 0.4$ meV is again found. In addition to the main peak, an extra side peak is observed at $U_{pg} = U^0_{pg} - \hbar\omega_\gamma$. The existence of this side peak is due to the formation of the one photon replica of the first excited state.

In the case of $\hbar\omega_\gamma > \hbar\omega_c$, where $\hbar\omega_\gamma = 0.3$ meV and $\hbar\omega_c \simeq 10^{-4}$ meV, the photon field is dominant. Comparing to the charge current in the absence of the cavity shown in Fig. 3(a) (blue solid), the current is increased in the main peak at $U^0_{pg} = 0.4$ mV which attributes to the fact that the charge density is stretched out of the QD, as shown in Fig. 4(b). This stretching effect is caused by the paramagnetic term of the electron–photon interaction. In addition, the contribution of the photon replica state with two photons can also enhance the charge current. It is worth mentioning that this happens because the energy of two photon replica state is higher than that of the first excited state in the energy spectrum. The higher states in the energy spectrum are less bound in the system and actively contribute to the electron transport.

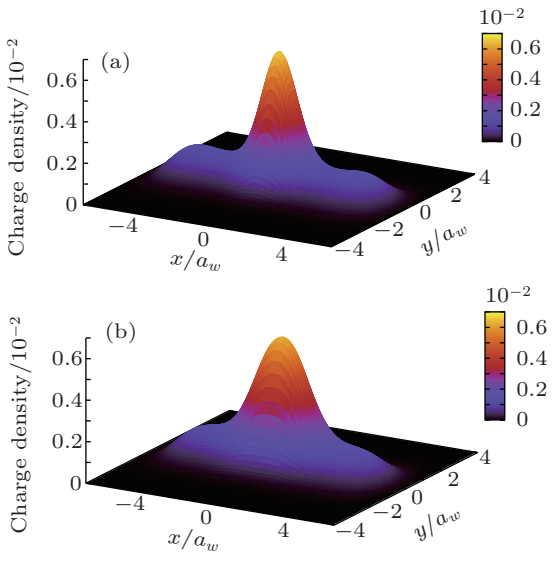


Fig. 4. (color online) Charge density in the QD system at $t = 220$ ps without (a) and with (b) photon cavity in the main current peak at $U^0_{pg} = 0.4$ mV shown in Fig. 3 for the cyclotron energy $\hbar\omega_c = 10^{-4}$ meV. The effective magnetic length is $a_w = 33.72$ nm, $\hbar\omega_\gamma = 0.3$ meV, $g_\gamma = 0.1$ meV, and $N_\gamma = 2$.

We should also note that the current is almost unchanged when $\hbar\omega_\gamma \simeq \hbar\omega_c$ (green dashed) with $\hbar\omega_c \simeq 0.34$ meV at the main peak recapturing the same value of current as was found in the absence photon cavity.

In addition, when $\hbar\omega_\gamma < \hbar\omega_c$ (red dotted line in Fig. 3(b)) with $\hbar\omega_c \simeq 0.86$ meV, the magnetic field effect is dominant. At this high cyclotron energy, the energy spacing between photon replica states is increased and the photon replica states weakly contribute to the electron transport. As a result, the charge current is decreased in the main peak.

Another interesting aspect of this issue is the influence of the external magnetic field on the current in the side peak displayed in Fig. 3(b). The formation of side peak is totally due to the photon cavity. It can be clearly seen that the current is high at low cyclotron energy when $\hbar\omega_\gamma > \hbar\omega_c$ (blue solid), indicating that the photon-induced current should be generated at low magnetic field. There are two reasons for the high current here: the photon replica states are more active in the electron transport at low cyclotron energy, and the stretching of charge density in the QD system due to the photon cavity. To explain the enhancement of current at the side peak, the charge density at $U_{pg} = 0.1$ mV is shown in Fig. 5 for the low cyclotron energy ($\hbar\omega_c \simeq 10^{-4}$ meV), i.e., $\hbar\omega_\gamma > \hbar\omega_c$, and the high cyclotron energy ($\hbar\omega_c \simeq 0.86$ meV), i.e., $\hbar\omega_\gamma < \hbar\omega_c$. In Fig. 5(a) the charge density is mostly distributed outside the QD and near the contact area to the leads. The charge accumulation in the contact area leads to the stronger charging to the QD system from the leads, and then the charge current at the side peak is increased. Therefore, we emphasize that the PAT process requires the following condition $\hbar\omega_\gamma > \hbar\omega_c$.

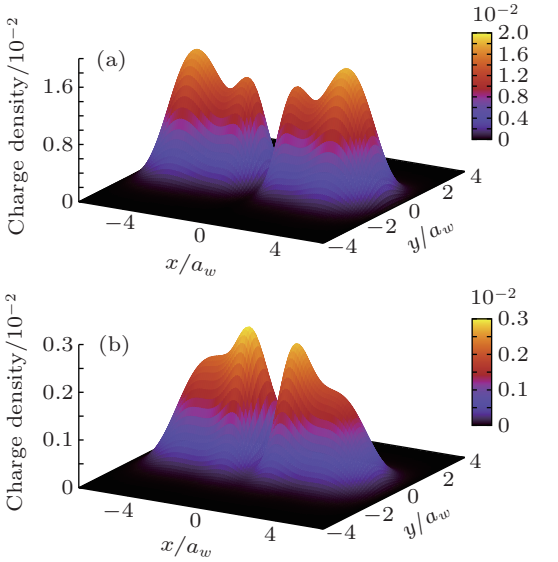


Fig. 5. (color online) Charge density in the QD system at $t = 220$ ps with photon cavity in the side current peak at $U_{pg} = 0.1$ mV shown in Fig. 3(b) for the case of $\hbar\omega_\gamma > \hbar\omega_c$ (a) and $\hbar\omega_\gamma < \hbar\omega_c$ (b). The effective magnetic length is $a_w = 33.72$ nm, $\hbar\omega_\gamma = 0.3$ meV, $g_\gamma = 0.1$ meV, and $N_\gamma = 2$.

By contrast, at high cyclotron energy ($\hbar\omega_c \simeq 0.86$ meV) when $\hbar\omega_\gamma < \hbar\omega_c$, the magnetic field dominates the electron

transport. The magnetic field causes the charge accumulation around the QD, as shown in Fig. 5(b), and then the current is reduced at the side peak.

4. Conclusions

We have investigated the influence of a static magnetic field on photon-induced transport through a QD coupled to a quantized photon cavity. It was found that the cavity forms photon replica states and their contribution to the electron transport can be affected by the external magnetic field. Therefore, two different regimes are studied, low and high magnetic fields. At the low magnetic field regime (low cyclotron energy), where the cyclotron energy is assumed to be lower than the photon energy, the photon replica states formed in the presence of the cavity actively contribute to the transport. Consequently, the charge density in the system are stretched and then the current is increased.

On the other hand, at the high magnetic field regime (high cyclotron energy), when the cyclotron energy is higher than the photon energy, the magnetic field is dominant and the photon-induced current is suppressed. As a result, we emphasis that the photon-induced transport or photon-assisted transport can be obtained when the photon energy is higher than the cyclotron energy in the system.

Acknowledgments

We acknowledge the Icelandic Research and Instruments Funds for financial support, and the Research Fund of the University of Iceland. The calculations were carried out on the Nordic High Performance Computer Center in Iceland. We are thankful to Dr. Peshwaz Abdoul for very interesting discussions. We acknowledge the Nordic network NANOCONTROL, and the University of Sulaimani.

References

[1] Imamoglu A and Yamamoto Y 1994 *Phys. Rev. Lett.* **72** 210
[2] Loss D and DiVincenzo D P 1998 *Phys. Rev. A* **57** 120
[3] DiVincenzo D P 2005 *Science* **309** 2173
[4] Petroff P M, Schmidt K H, Ribeiro G M, Lorke A and Kotthaus J 1997 *Jpn J. Appl. Phys.* **36** 4068
[5] Kouwenhoven L P and McEuen P L *Single Electron Transport Through a Quantum Dot*, in *Nanotechnology*, (ed. Gregory Timp) (New York: Springer) pp. 471–535
[6] Fujisawa T, van der Wiel W G and Kouwenhoven L P 2000 *Physica E* **7** 413
[7] Kouwenhoven L P, Jauhar S, McCormick K, Dixon D, McEuen P L, Nazarov Yu V, van der Vaart N C and Foxon C T 1994 *Phys. Rev. B* **50** 2019
[8] Shibata K, Umeno A, Cha K M and Hirakawa K 2012 *Phys. Rev. Lett.* **109** 077401
[9] Ishibashi K and Aoyagi Y 2002 *Physica B* **314** 437
[10] Kouwenhoven L P, Jauhar S, Orenstein J, McEuen P L, Nagamune Y, Motohisa J and Sakaki H 1994 *Phys. Rev. Lett.* **73** 3443
[11] Guo Y J and Nie W J 2015 *Chin. Phys. B* **24** 094205
[12] Ye H, Peng Y W, Yu Z Y, Zhang W and Liu Y M 2015 *Chin. Phys. B* **24** 114202
[13] Maksym P A and Chakraborty T 1990 *Phys. Rev. Lett.* **65** 108
[14] van der Wiel W G, De Franceschi S, Elzerman J M, Fujisawa T Tarucha S and Kouwenhoven L P 2002 *Rev. Mod. Phys.* **75** 1
[15] Thomas I 2010 *Semiconductor Nanostructures* (New York: Oxford University Press)
[16] Abdullah N R, Tang C S and Gudmundsson V 2010 *Phys. Rev. B* **82** 195325
[17] Hagenmüller D and Ciuti C *Phys. Rev. Lett.* 109 267403
[18] Maissen C, Scalari G, Valmorra F, Beck M, Faist J, Cibella S, Leoni R, Reichl C, Charpentier C and Wegscheider W 2014 *Phys. Rev. B* **90** 205309
[19] Abdullah N R 2015 *Cavity-photon Controlled Electron Transport through Quantum Dots and Waveguide Systems* (PhD Thesis: University of Iceland, Reykjavik, Iceland)
[20] Nakajima S 1958 *Prog. Theor. Phys.* **20** 948
[21] Zwanzig R 1960 *J. Chem. Phys.* **33** 1338
[22] Abdullah N R, Tang C S, Manolescu A and Gudmundsson V 2016 *ACS Photonics* **3** 249